

Can pretreatment hepatic artery perfusion scintigraphy in patients with liver malignancies predict the treatment response of the selective internal radiation therapy with ^{90}Y resin microspheres?

Isa Burak Guney 

Huseyin Tugsan Balli 

Kadir Alper Kucuker 

Ilker Unal 

Mustafa Kibar 

PURPOSE

We aimed to evaluate whether the perfusion pattern from pretreatment hepatic artery perfusion scintigraphy (HAPS) in patients with liver malignancies can predict response to selective internal radiation therapy (SIRT).

METHODS

This retrospective study analyzed 152 consecutive patients treated with yttrium-90 (^{90}Y) resin microspheres between April 2015 and July 2017. HAPS using single-photon emission computed tomography/computed tomography (SPECT/CT) with $^{99\text{m}}\text{Tc}$ macroaggregated albumin ($^{99\text{m}}\text{Tc}$ -MAA) was performed before SIRT. Investigators visually classified perfusion patterns of tumors as heterogeneous or diffuse in HAPS. Between diffuse and heterogeneous pattern group, positron emission tomography/computed tomography (PET/CT) and magnetic resonance imaging (MRI) were performed in third and sixth month after SIRT, and tumor response assessed and compared by using RECIST 1.1 or mRECIST. Overall survival (OS) and progression-free survival (PFS) were also compared with Kaplan-Meier/log-rank analyses.

RESULTS

Of 216 SIRT procedures, 172 were classified as heterogeneous and 44 as diffuse. Diffuse $^{99\text{m}}\text{Tc}$ -MAA uptake was associated with longer median OS than heterogeneous (22.2 vs. 14.4 months, respectively; $P = .047$). Subsegmental infusion was associated with longer OS than either lobar or segmental infusion ($P = .090$). Mean estimated OS was longer in patients with hepatocellular carcinoma (HCC) (34.2 months) than with colorectal carcinoma (CRC) (16.4 months) ($P = .044$). Patients with both diffuse and heterogeneous patterns were able to show complete response after SIRT. No statistically significant differences were observed between perfusion patterns and PFS or response rates to SIRT.

CONCLUSION

Although tumor perfusion patterns from preplanning HAPS analyses are useful for estimating tumor uptake of ^{90}Y , they may not reliably predict hepatic treatment response, as patients with different perfusion patterns can show clinical response to SIRT.

Selective internal radiation therapy (SIRT) with yttrium-90 (^{90}Y)-labeled microspheres has shown promising results in the treatment of patients with unresectable primary and metastatic liver cancer.^{1,2} SIRT takes advantage of the dual blood supply of liver; while the normal liver mostly receives blood from the portal vein, liver tumor neovascularization mainly originates from the hepatic artery. Targeted administration of ^{90}Y microspheres through the hepatic artery can deliver high doses of radiation to hepatic tumors with minimal exposure to healthy liver parenchyma.³ Hemodynamic flow within the hepatic arterial system and tumor vasculature affect microsphere distribution, as well as activity and delivered dose of ^{90}Y .⁴

Evaluating intratumoral heterogeneity with functional molecular imaging can predict the behavior of malignant tumors and eventual treatment response. Heterogeneity of uptake among metastatic lesions is influenced by factors such as cellular hypoxia, necrosis, vascularization, and proliferation—all which affect treatment response.^{5,6} Assessment of tumor perfusion is an essential preparatory step in SIRT to predict ^{90}Y microsphere distribution. A pretreatment planning angiography maps the hepatic and tumor vasculature and identifies

From the Departments of Nuclear Medicine (I.B.G. isaburak@gmail.com, K.A.K., M.K.), Radiology (H.T.B.), and Biostatistics (I.U.), Faculty of Medicine, Cukurova University, Adana, Turkey.

Received 19 August 2020; revision requested 17 September 2020; last revision received 1 December 2020; accepted 1 December 2020.

Published online 11 February 2022.

DOI: 10.5152/dir.2022.20775

You may cite this article as: Guney IB, Balli HT, Kucuker KA, Unal I, Kibar M. Can pretreatment hepatic artery perfusion scintigraphy in patients with liver malignancies predict the treatment response of the selective internal radiation therapy with ^{90}Y resin microspheres? *Diagn Interv Radiol.* 2022;28(2):156-165.

any potential off-target perfusion so that off-target ^{90}Y uptake can be prevented with prophylactic vessel embolization.⁷ Subsequent hepatic artery perfusion scintigraphy (HAPS) with $^{99\text{m}}\text{Tc}$ macroaggregated albumin ($^{99\text{m}}\text{Tc}$ -MAA) single-photon emission computed tomography/computed tomography (SPECT/CT) imaging is performed to simulate ^{90}Y microsphere injection. This imaging 1) detects and quantifies pulmonary shunting, 2) identifies extrahepatic uptake, and 3) determines the tumor-to-liver uptake ratio (TLR).⁸⁻¹¹ TLR is defined as the blood flow distribution ratio between the tumor and normal liver compartments and is an index of tumor-targeting effectiveness.¹² Because the size of $^{99\text{m}}\text{Tc}$ -MAA particles is comparable to that of ^{90}Y microspheres (25-35 microns), they should be distributed similarly when injected into the hepatic arterial vasculature and liver tissue, though differences can exist. This association can indicate the relative density of the hepatic microvascular structure and identify the associated areas of deposition.^{3,9} Therefore, distribution of $^{99\text{m}}\text{Tc}$ -MAA activity is a measure of expected ^{90}Y microsphere activity distribution and thus estimated radiation dose received.

Studies investigating the value of assessing pre-SIRT $^{99\text{m}}\text{Tc}$ -MAA perfusion patterns for predicting ^{90}Y distribution/dosimetry and tumor response had mixed results.¹³⁻¹⁵ One study described a semiquantitative imaging approach involving positron emission tomography/computed tomography (PET/CT),

SPECT, and CT scans in patients with liver metastases from colorectal cancer (CRC). Using a cutoff value of 1 for the $^{99\text{m}}\text{Tc}$ -MAA TLR, the authors predicted the post-SIRT metabolic response with a sensitivity of 89%, specificity of 65%, positive predictive value of 71%, and negative predictive value of 87%.¹³ Another study in patients with metastatic CRC used magnetic resonance imaging (MRI) to evaluate the association between $^{99\text{m}}\text{Tc}$ -MAA uptake and response to SIRT and found no significant correlation. Because patients with low $^{99\text{m}}\text{Tc}$ -MAA uptake showed significant response to therapy, the authors advised against excluding patients from SIRT who lacked scintigraphic $^{99\text{m}}\text{Tc}$ -MAA accumulation.¹⁴ A retrospective analysis that assessed $^{99\text{m}}\text{Tc}$ -MAA uptake with HAPS in 80 patients with mixed tumor diagnoses reported a correlation between type of perfusion pattern and tumor response, although response was the sole measure of SIRT efficacy.¹⁵

Considering that tumor vascularization and the tumor-to-normal arterial blood flow ratio may vary considerably among patients and tumor types, heterogeneous treatment responses and perfusion patterns are expected. Varied tumor vasculature may result in heterogeneous or diffuse HAPS perfusion patterns.¹⁶ Hypervascular tumors are expected to concentrate ^{90}Y microspheres more efficiently and respond better to SIRT than hypovascular tumors. However, high tumor vascularization indicated by HAPS may not necessarily be a prerequisite for successful SIRT, as an inverse correlation between $^{99\text{m}}\text{Tc}$ -MAA accumulation and patient

survival has been reported. Extensive tumor vascularization may be accompanied by particularly aggressive tumor biology that manifests regardless of tumor dose.¹⁶ Thus, a reliable model to predict SIRT efficacy remains elusive. We hypothesized that heterogeneous perfusion of $^{99\text{m}}\text{Tc}$ -MAA may reflect tumor heterogeneity, which might lead to different treatment response than diffuse perfusion reflecting tumor homogeneity. This study investigated the associations between tumor perfusion visualized with pre-paratory HAPS SPECT/CT imaging, patient survival, and tumor response to SIRT assessed using fluorine-18 fluorodeoxyglucose (^{18}F -FDG) PET/CT and abdominal MRI in a large population (152 patients and 216 SIRT procedures). We also considered the role of tumor vascularity and method of SIRT administration.

Methods

Patients from a single institution treated with ^{90}Y resin microspheres (SIR-Spheres[®], Sirtex Medical Limited) between April 2015 and July 2017 were retrospectively analyzed. Eligible patients had unresectable liver-dominant disease, adequate hepatic reserve (albumin > 3.0 g/dL, total bilirubin < 2mg/dL), and Eastern Cooperative Oncology Group (ECOG) performance status of 0-2. All patients provided written informed consent for SIRT. All procedures performed in studies involving human participants were in accordance with the ethical standards of the institutional and/or national research committee and with the 1964 Helsinki declaration and its later amendments or

Main points

- Post-SIRT dosimetry with bremsstrahlung SPECT/CT is good complementary evaluation to confirm HAPS findings.
- The diffuse pattern of HAPS is associated with higher complete response rate than heterogeneous pattern. But, it should be kept in mind that lower stage and smaller tumors in diffuse pattern group contributes to this result.
- No significant difference was found between diffuse and heterogeneous uptake patterns for overall, objective and hepatic response rates.
- Hypervascular tumors are significantly associated with higher overall, objective and hepatic response rates than hypovascular tumors.
- SIRT is a useful option for treating liver tumors in both diffuse and heterogeneous activity distribution patterns.

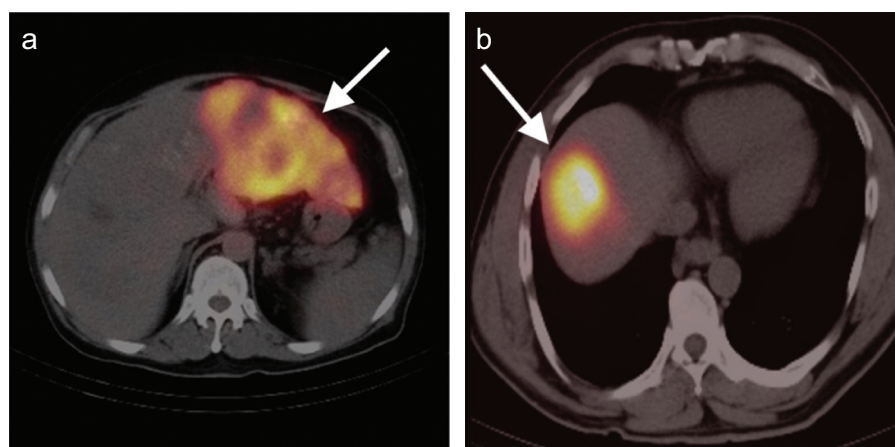


Figure 1. a, b. Tumor perfusion patterns in hepatic artery perfusion scintigraphy (HAPS) single-photon emission/computed tomography (SPECT/CT) scans: (a) heterogeneous pattern, (b) diffuse pattern (arrows).

Table 1. Patient demographics and baseline characteristics stratified according to the liver perfusion patterns detected with HAPS scans in all performed SIRT procedures

| | ^{99m} Tc-MAA perfusion pattern | | P |
|---------------------------------------|---|------------------------------------|-------|
| | Heterogeneous, n = 172 | Diffuse, n = 44 | |
| Age (years), mean ± SD | 59.5 ± 12.2 (1-86) | 58.4 ± 10.7 (38-75) | .562 |
| Sex, n(%) | | | .917 |
| Male | 108 (62.8) | 28 (63.6) | |
| Female | 64 (37.2) | 16 (36.4) | |
| Tumor type, n (%) | | | <.001 |
| HCC | 52 (30.2) | 16 (36.4) | |
| CRC | 51 (29.7) | 4 (9.1) | |
| CCC | 30 (17.4) | 3 (6.8) | |
| Breast | 17 (9.9) | 4 (9.1) | |
| NET | 2 (1.2) | 12 (27.3) | |
| Stomach | 6 (3.5) | 2 (4.5) | |
| Pancreas | 4 (2.3) | 1 (2.3) | |
| Gallbladder | 3 (1.7) | 0 (0.0) | |
| GIST | 2 (1.2) | 1 (2.3) | |
| Hepatoblastoma | 2 (1.2) | 0 (0.0) | |
| Ovarian | 2 (1.2) | 0 (0.0) | |
| Sarcoma | 1 (0.6) | 1 (2.3) | |
| Tumor size (cm), n (%) | | | <.001 |
| <2 | 1 (0.6) | 2 (4.5) | |
| 2-5 | 63 (36.6) | 28 (63.6) | |
| >5 | 108 (62.8) | 14 (31.8) | |
| PVTT | 16 (9.3) | 2 (4.5) | .540 |
| Prior treatment, n (%) | | | |
| None | 33 (19.2) | 5 (11.4) | |
| Surgery | 4 (2.3) | 0 (0.0) | |
| Chemotherapy | 63 (36.6) | 7 (15.9) | |
| TACE + RF + MW | 12 (7.0) | 8 (18.2) | |
| SIRT | 4 (2.3) | 1 (2.3) | |
| Sorafenib | 8 (4.7) | 3 (6.8) | |
| Sorafenib + SIRT | 6 (3.5) | 1 (2.3) | |
| SIRT + TACE + CT | 42 (24.4) | 19 (43.2) | |
| Tumor markers, mean±SD (range) | | | |
| AFP (IU/mL) | | | |
| Baseline ^a | 4179.6 ± 12120.1 (0.20-81846.0) | 17381.4 ± 60515.6 (0.90-250.413.0) | .624 |
| 3 months ^a | 6882.7 ± 34764.4 (1.70-247933.0) | 1900.3 ± 6948.4 (1.40-28807.0) | .348 |
| CEA (U/mL) | | | |
| Baseline ^b | 511.2 ± 2813.6 (0.57-21054.35) | 22.1 ± 67.9 (1.04-284.74) | .023 |
| 3 months ^b | 789.4 ± 4227.9 (0.64-29146.41) | 6.8 ± 7.4 (1.12-24.57) | .026 |
| CA 19-9 (ng/dL) | | | |

Table 1. Patient demographics and baseline characteristics stratified according to the liver perfusion patterns detected with HAPS scans in all performed SIRT procedures (Continued)

| | ^{99m} Tc-MAA perfusion pattern | | P |
|-----------------------|---|----------------------------|------|
| | Heterogeneous, n = 172 | Diffuse, n = 44 | |
| Baseline ^b | 8456.9 ± 35505.9 (0.80-200.300.0) | 82.7 ± 124.9 (0.80-465.60) | .342 |
| 3 months ^b | 1715.8 ± 7816.2 (0.80-66.820.0) | 54.0 ± 56.5 (0.80-168.90) | .168 |

^aHCC and CCC patients.

^bCCC patients only.

HAPS, hepatic artery perfusion scintigraphy; SIRT, selective internal radiation therapy; Tc-MAA, technetium macroaggregated albumin; HCC, hepatocellular carcinoma; CRC, colorectal cancer; CCC, cholangiocellular carcinoma; NET, neuroendocrine tumors; GIST, gastrointestinal stromal tumor; PVTT, portal vein tumor thrombosis; TACE, transarterial chemoembolization; RF, radiofrequency ablation; MW, microwaves; CT, computed tomography; AFP, alpha-fetoprotein; CEA, carcinoembryonic antigen; CA 19-9, carbohydrate antigen 19-9.

Table 2. SPECT/CT pretreatment planning measures stratified according to the liver perfusion patterns detected with HAPS scans performed before all SIRT procedures

| | | |
|--------------------------------------|---------------------------|-------------------------|
| LSF (%) | 6.8 ± 5.12 (0-20) | 4.98 ± 3.84 (0-16) |
| TLR | 1.78 ± 1.86 (0-6) | 1.99 ± 2.06 (0-5) |
| Y-90 activity (mBq) | 1221.0 ± 569.8 (370-3700) | 1054 ± 488.4 (370-2997) |
| Tumor absorbed dose (Gy) | 191.0 ± 70.4 (54-404) | 250.6 ± 78.8 (106-400) |
| Normal parenchyma-absorbed dose (Gy) | 46.6 ± 11.7 (14-75) | 55.9 ± 11.9 (36-83) |
| Lung absorbed dose (Gy) | 4.11 ± 4.63 (0.3-24) | 2.34 ± 1.72 (0.3-8.3) |

SPECT/CT, single-photon emission computed tomography; HAPS, hepatic artery perfusion scintigraphy; SIRT, selective internal radiation therapy; LSF, lung shunt fraction; TLR, tumor-to-liver ratio.

comparable ethical standards. For this type of study, formal consent is waived. This study was approved by Ethical Committee of our institution (31.08.2018/80).

All patient cases were reviewed prior to treatment by an interdisciplinary tumor board that included a medical oncologist, gastroenterologist, interventional radiologist, radiation oncologist, surgeon, and nuclear medicine expert. Before SIRT, all patients underwent routine laboratory analyses, including a complete blood count and tests for liver and renal function and coagulation. Levels of disease-specific tumor markers were measured for primary liver malignancies; markers included alpha-fetoprotein (AFP) for hepatocellular carcinoma (HCC) and carbohydrate antigen 19-9, AFP, and carcinoembryonic antigen for cholangiocellular carcinoma (CCC).

Pretreatment planning angiography and HAPS SPECT/CT

HAPS SPECT/CT was performed in all patients following the standard pretreatment hepatomesenteric angiography and C-arm cone-beam CT to assess tumor vasculature.⁸ The ^{99m}Tc-MAA (Pulmocis[®], IBA Molecular)

(10-90 μm particles) was prepared immediately before the scan and injected into a hepatic artery branch feeding the target region through a percutaneous catheter. The injection activity, concentration, and final volume were 148 MBq (4 mCi), 100,000 particles/mL, and 4 mL, respectively. SPECT/CT imaging acquisition was started within 45 minutes of the ^{99m}Tc-MAA injection. Oral sodium perchlorate was administered before the procedure to avoid formation of ^{99m}Tc-MAA degradation-related artifacts that could potentially generate false activity.¹⁷ Uptake of ^{99m}Tc-MAA was captured with a dual-head gamma camera equipped with low-energy, ultra-high-resolution collimators (Symbia T16, Siemens Healthcare). SPECT acquisition parameters were peak energy 140 keV (window: 20%), step-and-shoot protocol, and 25 s/projection at 256 × 256 matrix. CT acquisition parameters were 10 mm axial sampling, 140 kVp, 2.5 mA, and 256 × 256 matrix size.

Tumor and treatment area volumes were calculated from angiogram and SPECT/CT fusion images using OsiriX MD software (Pixmeo SARL), which allowed investigators to manually select regions of interest (ROI).

Total tumor volume for each patient was calculated as the sum of the volumes of all selected lesions. Treatment area volume corresponded to ^{99m}Tc-MAA distribution area, defined as the sum of the tumor area and the normal parenchyma area with ^{99m}Tc-MAA uptake. In necrotic tumors, volume of the area of low uptake was not analyzed.

HAPS images were evaluated visually by one of the authors, and tumor perfusion pattern was classified as heterogeneous or diffuse (Figure 1). In diffuse patterns, MAA particles are distributed almost uniformly within the treatment area, including the tumor, with no hypoactive areas. In contrast, heterogeneous patterns show a less-uniform distribution, often with hypoactive areas.

SIRT and postprocedure treatment response evaluation

The partition model was used to calculate ⁹⁰Y activity and the dose to administer to each patient.^{18,19} SIRT was performed in accordance with standard methods.⁸

In accordance with procedure standards, ⁹⁰Y microspheres were infused through the hepatic artery using three different approaches: lobar, segmental, or subsegmental (via direct tumor-feeding vessels).²⁰ Subsegmental therapy was performed in patients with solitary lesions to allow ⁹⁰Y microsphere delivery. Segmental infusion was performed in patients with a tumor (either primary or metastatic) localized in a distinct liver segment supplied by a single segmented branch of the hepatic artery, which was identified and catheterized. In patients with bilobar disease, each lobe was treated sequentially at 4- to 6-week intervals to maintain a degree of functional capacity in

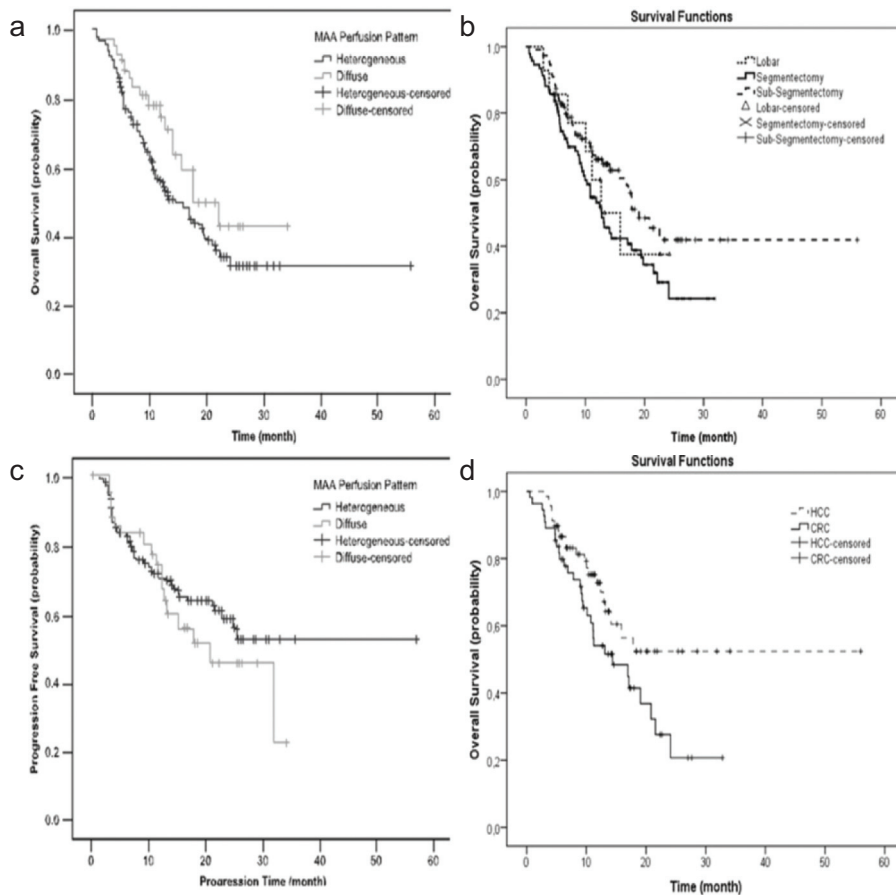


Figure 2. a-d. Overall survival. (a) A diffuse perfusion pattern was associated with a longer median OS than a heterogeneous pattern ($P = .047$). (b) There was no statistical difference between heterogeneous and diffuse patterns in terms of progression-free survival ($P = .743$). (c) The median OS associated with subsegmental infusion was greater than the median OS for either lobar or segmental infusion ($P = .090$). (d) Patients with HCC had a longer mean OS than those with CRC ($P = .044$). CRC, colorectal cancer; HCC, hepatocellular carcinoma; MAA, macroaggregated albumin; OS, overall survival.

the contralateral lobe. These patients were assessed 4 weeks after the first ^{90}Y microsphere administration to decide whether to proceed with the second treatment.

Postprocedure ^{90}Y -bromsstrahlung SPECT/CT scan was performed with medium-energy all-purpose collimators (energy window, $160 \text{ keV} \pm 30\%$; matrix, 128×128 ; 6° steps; 40 s/frame) and reconstructed using an iterative method. Attenuation correction was applied to both $^{99\text{m}}\text{Tc}$ -MAA and ^{90}Y SPECT/CT.

After SIRT, all patients were prescribed a proton pump inhibitor and steroid, analgesic, and antiemetic drugs. Because ^{90}Y is a pure beta emitter, isolation for radioprotection was not necessary after treatment. Although the radiation hazard presented by patients to other people is very low, traces of ^{90}Y can be detected in urine; all patients received complete instructions about radiation safety precautions.

Patient follow-up

To evaluate therapy response 3 and 6 months after SIRT, patients underwent hepatocyte-specific, contrast-enhanced MRI (Ingenia 3.0T MR System, Philips; and Signa HDi EchoSpeed 1.5T, GE Healthcare) and ^{18}F -FDG PET/CT (Biograph 6, Siemens Medical Systems). The findings acquired with third and sixth months imagings were compared with initial ^{18}F -FDG PET/CT and contrast-enhanced MRI according to therapy response criteria.

The European Organization for Research and Treatment of Cancer criteria (EORTC) and Response Evaluation Criteria in Solid Tumors (RECIST) were used to assess tumor response to SIRT in ^{18}F -FDG PET/CT images based on baseline-chosen, lesion-specific ROIs observed on each scan.²¹ The RECIST version 1.1 or modified RECIST criteria were used to evaluate tumor response in MRI images of hypovascular and hypervascular

tumors. Hypervascular tumors have increased intensity on arterial- or portal-phase images on dynamic contrast-enhanced MRI.

Because distant metastases can occur during follow-up despite a primary tumor response, multiple response endpoints were considered. Objective response was evaluated only in treated lesions, whereas overall response was analyzed in both hepatic and extrahepatic lesions. Hepatic response was evaluated in all lesions in both liver lobes, regardless of treatment with SIRT.

Statistical analysis

Analyses were performed using the IBM SPSS Statistics Solution, version 20.0 (IBM) software package. Progression-free survival (PFS) and overall survival (OS) were calculated from the first HAPS procedure date for all patients, considered as the baseline date. Categorical variables were expressed as numbers and percentages, and continuous variables as mean and standard deviation or median and range, where appropriate. The chi-square test and Mann-Whitney U test were used to compare categorical and continuous variables, respectively. For comparison of categorical variables, Fisher exact test was applied if the expected cell count was small. For survival analysis, OS was calculated using the Kaplan-Meier method, and the Log rank test was used to compare Kaplan-Meier curves. The threshold for statistical significance for all tests was $P < .05$.

Results

Overall, 216 HAPS/SIRT procedures were performed in 152 patients. Table 1 represents the characteristics of patient group according to the liver perfusion patterns in HAPS (Table 1). Patients had an ECOG performance status of 0 ($n = 127$, 83.6%) or 1 ($n = 25$, 16.4%). Twenty-four SIRT procedures were performed in patients with HCC and portal vein tumor thrombosis (PVTT); follow-up data were available for 18/24 patients. The HAPS pretreatment planning measures were determined and stratified by perfusion pattern (Table 2).

Four patients were not treated because they had LSF $> 20\%$ and were excluded from analyses. Overall, 14 lobar, 92 segmental, and 110 subsegmental ^{90}Y infusion SIRT procedures were performed. To increase the tumor-to-liver dose ratio, 12/92

Table 3. MAA perfusion pattern and MRI results or treatment type

| | | | MAA perfusion pattern | | |
|----------------|---------------|-------------------------|-----------------------|---------|-------|
| | | | Heterogeneous | Diffuse | Total |
| MRI pattern | Hypervascular | Count | 106 | 32 | 138 |
| | | % within MRI pattern | 76.8 | 23.2 | 100 |
| | | % within MAA pattern | 61.6 | 72.7 | 63.9 |
| | Hypovascular | Count | 66 | 12 | 78 |
| | | % within MRI pattern | 84.6 | 15.4 | 100 |
| | | % within MAA pattern | 38.4 | 27.3 | 36.1 |
| | Total | Count | 172 | 44 | 216 |
| | | % within MRI pattern | 79.6 | 20.4 | 100 |
| | | % within MAA pattern | 100 | 100 | 100 |
| Treatment type | Lobar | Count | 13 | 1 | 14 |
| | | % within treatment type | 92.9 | 7.1 | 100 |
| | | % within MAA pattern | 7.6 | 2.3 | 6.5 |
| | Segmental | Count | 74 | 18 | 92 |
| | | % within treatment type | 80.4 | 19.6 | 100 |
| | | % within MAA pattern | 43.0 | 40.9 | 42.6 |
| | Subsegmental | Count | 85 | 25 | 110 |
| | | % within treatment type | 77.3 | 22.7 | 100 |
| | | % within MAA pattern | 49.4 | 56.8 | 50.9 |
| | Total | Count | 172 | 44 | 216 |
| | | % within treatment type | 79.6 | 20.4 | 100 |
| | | % within MAA pattern | 100 | 100 | 100 |

MAA, macroaggregated albumin; MRI, magnetic resonance imaging.

patients who received radiation segmentectomy underwent protective coil embolization of the subsegmental branches supplying the normal parenchyma before SIRT. No patients showed any extrahepatic leakage during SIRT. We also performed right lobar treatment in 6 patients in whom the tumor covered almost the entire right lobe.

The mean interval between HAPS and SIRT was 11.7 ± 6 days (0-34), and mean follow-up time after SIRT was 12.1 ± 7.8 months (0.5-32.8). Twelve (7.9%) patients died before 3 months, and 32 (21%) patients died between the 3-month and 6-month follow-ups.

Heterogeneous and diffuse ^{99m}Tc -MAA uptake patterns were observed in 172 (79.6%) and 44 (20.4%) procedures, respectively. Estimated median OS for the heterogeneous pattern subgroup was 14.4 months (95% confidence interval [CI], 10.48-18.32) and for the diffuse pattern subgroup was 22.2 months (95% CI, 13.96-30.44) ($P = .047$)

(Figure 2a). No statistically significant differences were observed between perfusion pattern and PFS ($P = .743$) (Figure 2b).

Median OS estimated for the three different infusion methods was 12.6 months (95% CI, 6.5-18.8) for lobar, 12.7 months (95% CI, 9.8-15.6) for segmental, and 19.1 months (95% CI, 14.3-23.9) for subsegmental ($P = .090$) (Figure 2c). When the OS of the two most frequently encountered tumor types was analyzed, median OS could not be estimated for CRC because fewer than half of patients with CRC had died before the end of the follow-up period. We therefore compared the mean OS between the two groups, which was 34.2 months (95% CI, 26.9-41.5) in patients with HCC and 16.4 months (95% CI, 13.1-19.7) in patients with CRC ($P = .044$) (Figure 2d).

Tumor vascularity analysis of MRI images of all 216 procedures revealed 138 (63.9%) hypervascular and 78 (36.1%) hypovascular perfusion patterns (Table 3).

The majority of procedures (172/216) were associated with heterogeneous perfusion patterns. Diffuse pattern was least common with lobar treatment and most common with subsegmental treatment (Table 3). The percentage of solitary lesions (rather than multifocal) was higher in patients who underwent subsegmental (45.5%) and lobar (42.9%) procedures compared to segmental procedures (18.5%).

Of the 152 patients, 137 (90%) and 88 (56%) had imaging data available at the 3- and 6-month follow-ups, respectively. Diffuse and heterogeneous perfusion patterns were associated with different response rates. The diffuse pattern was associated with a significantly higher complete response (CR) rate than the heterogeneous pattern with both PET/CT and MRI, and at both the 3- and 6-month assessments ($P < .05$ for all comparisons; Figure 3). MRI evaluations at 3 months showed a higher partial response (PR) rate in patients with a heterogeneous pattern than in those with a diffuse pattern (58.6% vs. 40.0%; $P = .038$; Figure 3c).

Overall, no statistically significant differences were observed between heterogeneous and diffuse perfusion patterns for objective, overall, and hepatic response rates (CR + PR + stable disease [SD]) (Figure 3). Despite receiving higher ^{90}Y radiation activity (33.0 ± 15.4 vs. 28.5 ± 13.3 mCi), patients showing heterogeneous HAPS perfusion patterns had lower tumor-absorbed doses than patients with diffuse patterns (191.1 ± 70.4 vs. 250.6 ± 78.8 Gy, respectively; Table 2). This difference in lower absorbed dose was statistically significant ($P < .001$).

Of 18 analyzed patients with HCC and PVTT, 1 had CR (based on both PET/CT and MRI results), 13 had PR, 2 had SD, and 2 had progressive disease (not shown).

Hypervascular tumors were significantly associated with higher objective, overall, and hepatic response rates than hypovascular tumors, as observed in both 3- and 6-month PET/CT and MRI follow-up results ($P < .05$ for all but one comparison; Table 4).

Figure 4 shows an exemplary case of a patient with CRC who showed a heterogeneous perfusion pattern with a complete metabolic response at 3 months after SIRT. A bremsstrahlung image acquired after SIRT (Figure 4d) demonstrates a discrepancy with the HAPS image acquired before SIRT (Figure 4c).

Discussion

In this retrospective analysis, we evaluated the association between ^{99m}Tc -MAA uptake patterns observed in pre-SIRT HAPS scans and posttreatment OS, PFS, and tumor response assessed with MRI and ^{18}F -FDG PET/CT scans. We examined the correlation between perfusion pattern and factors such as ^{90}Y infusion method and tumor vascularity.

We found that a diffuse perfusion pattern was significantly associated with longer median OS than a heterogeneous pattern ($P = .047$). However, no other statistically significant association between perfusion and treatment efficacy (ie, PFS and objective, overall, and hepatic response rates) was observed. This suggests that although perfusion of ^{90}Y may influence treatment outcome, it is not the only factor determining treatment response. Our results are consistent with a previous retrospective analysis in 80 patients with primary and metastatic liver tumors,¹⁵ which found that diffuse or heterogeneous ^{99m}Tc -MAA HAPS perfusion patterns were a good predictor of early response to SIRT. The authors reported that a diffuse pattern was associated with better tumor response.¹⁵ However, OS and PFS were not evaluated, and the body surface area (BSA) formula was used to calculate ^{90}Y activity and administered dose. The commonly used BSA formula postulates that BSA correlates with the size of each patient's liver and tumor burden, but it neglects variabilities in tumor vascularity and tumor-to-normal ratio among patients.^{18,19} In this study, we calculated dose and activity of ^{90}Y using the partition model, a more accurate and personalized method based on Medical Internal Radiation Dose principles. This model hypothesizes that three distinct vascular compartments (lungs, tumor, and uninvolved liver parenchyma) can be partitioned during ^{90}Y microsphere infusion.^{18,19} We considered the partition model a more appropriate method to calculate ^{90}Y activity and dose according to the predicted microsphere distribution based on ^{99m}Tc -MAA HAPS scans.

Although heterogeneity of tumors has been demonstrated to predict treatment failure and drug resistance,⁵ our results included many instances in which patients with heterogeneous perfusion patterns, such as patient case 1 (Figure 4), showed positive responses to SIRT. We

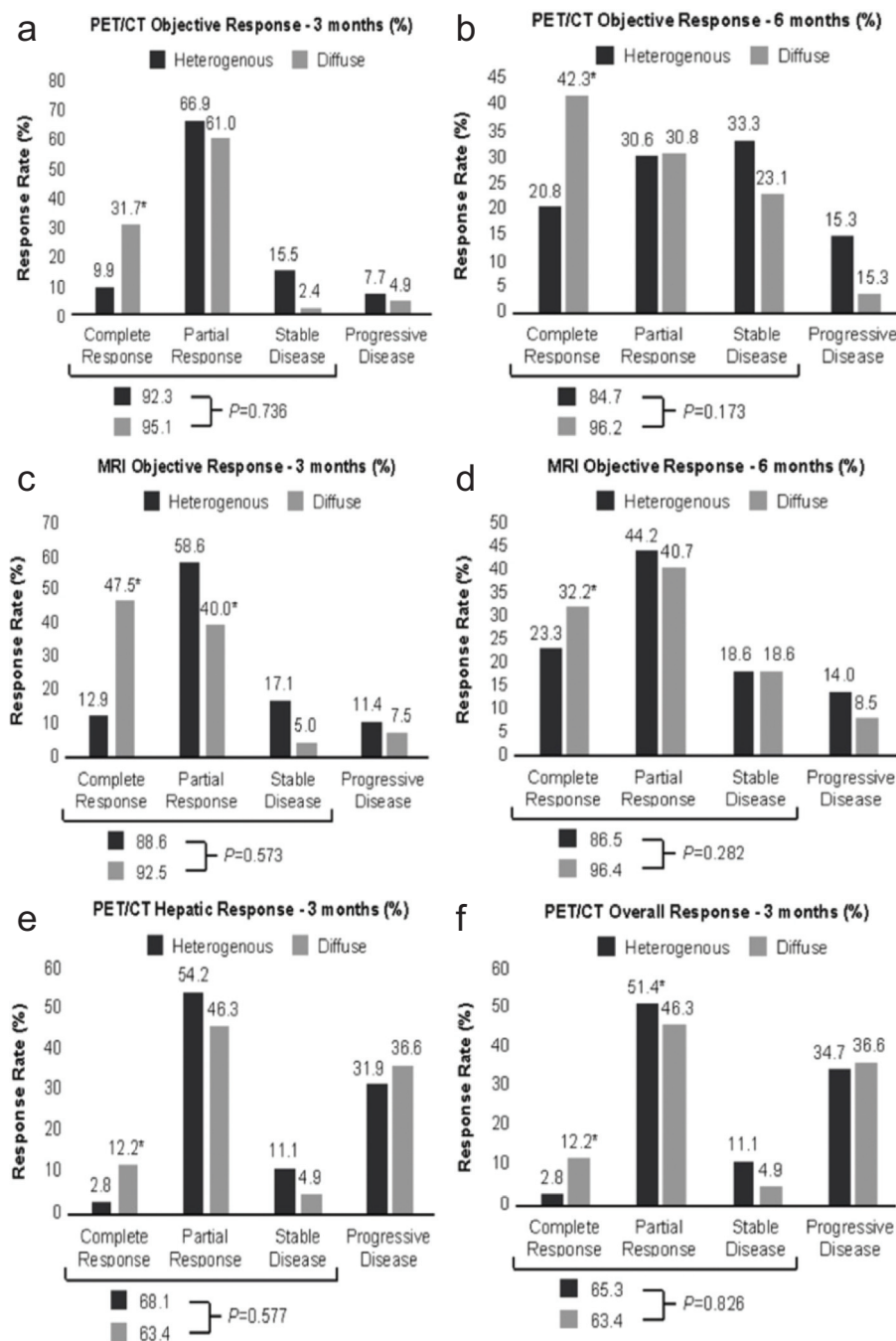


Figure 3. a-d. Objective response rates obtained with PET/CT (a, b) and MRI (c, d), 3 (a, c) and 6 (b, d) months after SIRT. (e, f): Hepatic (e) and overall (f) response rates obtained with PET/CT 3 months after SIRT. Results are shown for the subgroup populations with heterogeneous and diffuse ^{99m}Tc -MAA perfusion patterns in HAPS imaging results. Objective, overall, and hepatic response rates (CR + PR + SD) and relative P values associated with heterogeneous and diffuse perfusion patterns are shown below each histogram. CR, complete response; HAPS, hepatic artery perfusion scintigraphy; MRI, magnetic resonance imaging; PET/CT, positron emission tomography/computed tomography; PR, partial response; SD, stable disease; SIRT, selective internal radiation therapy; ^{99m}Tc -MAA, ^{99m}Tc macroaggregated albumin. * $P < .05$.

Fatigue, pain, nausea, vomiting, and fever were the most common adverse effects after treatment and were experienced in most patients to varying degrees. No grade 3 and 4 toxicities were

observed at the 3-month follow-up. In addition, no patients demonstrated any features of radiation-induced liver disease. No pulmonary toxicity was reported.

Table 4. Objective, overall, and hepatic response rates associated with hypervascular and hypovascular tumors

| Objective response ^a (CR + PR + SD), n (%) | | | |
|---|------------|-----------|------|
| 3-month follow-up | | | |
| PET/CT | 118 (95.9) | 52 (86.7) | .031 |
| MRI | 112 (92.6) | 49 (83.1) | .051 |
| 6-month follow-up | | | |
| PET/CT | 68 (93.2) | 18 (72.0) | .011 |
| MRI | 70 (90.9) | 21 (84.0) | .457 |
| Overall response ^b (CR + PR + SD), % | | | |
| 3-month follow-up | | | |
| PET/CT | 89 (71.8) | 31 (50.8) | .005 |
| Hepatic response ^c (CR + PR + SD), % | | | |
| 3-month follow-up | | | |
| PET/CT | 93 (75.0) | 31 (50.8) | .001 |

^aResponse in treated lesions.^bResponse in both hepatic and extrahepatic lesions.^cResponse in entire liver (both treated and untreated lesions).

CR, complete response; PR, partial response; SD, stable disease; PET/CT, positron emission tomography/computed tomography; MRI, magnetic resonance imaging

believe that patients should not be disqualified for SIRT solely based on perfusion pattern shown during preplanning HAPS analyses.

The largest subpopulation in the study had HCC. The benefits of SIRT in patients with HCC and PVTT have been demonstrated in two randomized controlled trials and one large retrospective analysis, in which higher tumor response rates (CR or PR), PFS and time to progression, and OS were compared in patients treated with SIRT or sorafenib.^{22–24} In our study, we showed that SIRT is an effective treatment option in patients with HCC and tumor-related PVTT, classified as advanced HCC Barcelona Clinic Liver Cancer stage C. Irrespective of tumor HAPS perfusion pattern, 16/18 patients with HCC and PVTT responded to SIRT.

Cumulative OS was almost twice as long in patients with HCC versus those with CRC (Figure 2d). This may be because patients with HCC who are candidates for superselective embolization naturally have better prognoses than those with metastatic refractory CRC who have already undergone several previous cycles of chemotherapy. Likewise, subsegmental treatment resulted in longer median OS than lobar or segmental treatment, although the difference was not statistically significant ($P = .090$) (Figure 2c). Livers undergoing lobar infusion might be more likely to show

heterogeneous distribution because they are more likely to contain multifocal tumors, whereas a subsegmental injection would most likely generate a diffuse pattern. Patients who undergo subsegmental infusion likely had a solitary lesion at baseline, whereas a larger number of segments were likely involved when lobar or segmental infusions were required. Indeed, the percentage of solitary lesions was higher in patients who underwent subsegmental treatment versus segmental treatment (45.5% vs. 18.5%). As a result, it is natural to detect diffuse perfusion pattern and to obtain better prognosis rates with subsegmental infusions due to lower stage disease and smaller tumor dimension. Therefore, this can be evaluated as selection bias for study group.

Despite receiving a higher ⁹⁰Y radiation dose than patients with a diffuse perfusion pattern, patients with a heterogeneous perfusion pattern showed a lower tumor-absorbed dose (Table 2). This may be because lesions that showed a heterogeneous pattern were more multifocal than those with a diffuse pattern and were treated more favorably using lobar or segmental (≥ 1) ⁹⁰Y SIRT instead of superselective subsegmental treatment. The rest of the dose may be absorbed by the normal parenchyma between multiple lesions.

The type of HAPS perfusion pattern is not the only parameter that affects clinical

outcomes of SIRT; other factors to consider include the relationship between tumor biology and vascularity, functional integrity of uninvolved hepatic parenchyma, and relative radiosensitivities of the tumor and normal liver. The radiation dose administered, tumor hemodynamics, and vascularity are among the main factors that affect tumor response to SIRT.⁴ Although tumor vascularity and degree of ^{99m}Tc-MAA uptake in pre-SIRT HAPS images cannot entirely explain SIRT efficacy, we reported significantly higher response rates in hypervascular tumors than in hypovascular tumors at both 3- and 6-month posttreatment time points and with both PET/CT and MRI imaging modalities.

Radiation segmentectomy is often used to treat liver tumors with unfavorable location or large size that prevents resection or ablation.²⁵ Radiation segmentectomy minimizes the volume of normal tissue exposed to radiation and maximizes the tumor-delivered ⁹⁰Y dose. A dose restriction for normal liver parenchyma is not required when using this method. There is little published evidence on ⁹⁰Y microspheres and radiation segmentectomy. In our study, 93 patients underwent radiation segmentectomy, and all showed good treatment responses, even in patients with heterogeneous perfusion.

SIRT has been shown to effectively downstage patients with different primary tumors or liver metastases for subsequent transplantation²⁶ or surgical resection.²⁷ In our study, SIRT was successfully used as a bridge to transplantation in three patients with HCC, and as a bridge to resection in two patients with HCC. SIRT was effective in downstaging tumors for resection and transplantation in patients with diverse tumor perfusion patterns.

We evaluated intratumoral heterogeneity visually from MAA perfusion patterns and classified each pattern as heterogeneous or diffuse. Some other interesting quantitative approaches are available to measure heterogeneity in metastatic tumors. For example, FDG metabolism can be used to generate a heterogeneity index by measuring the maximum or average standardized uptake value (SUVmax or SUVmean).²⁸ In our study, ¹⁸F-FDG PET/CT facilitated the selection of patients for surgical resection or liver transplantation, though it was only used after SIRT. In addition to radiological images of the abdomen that evaluate treatment response after

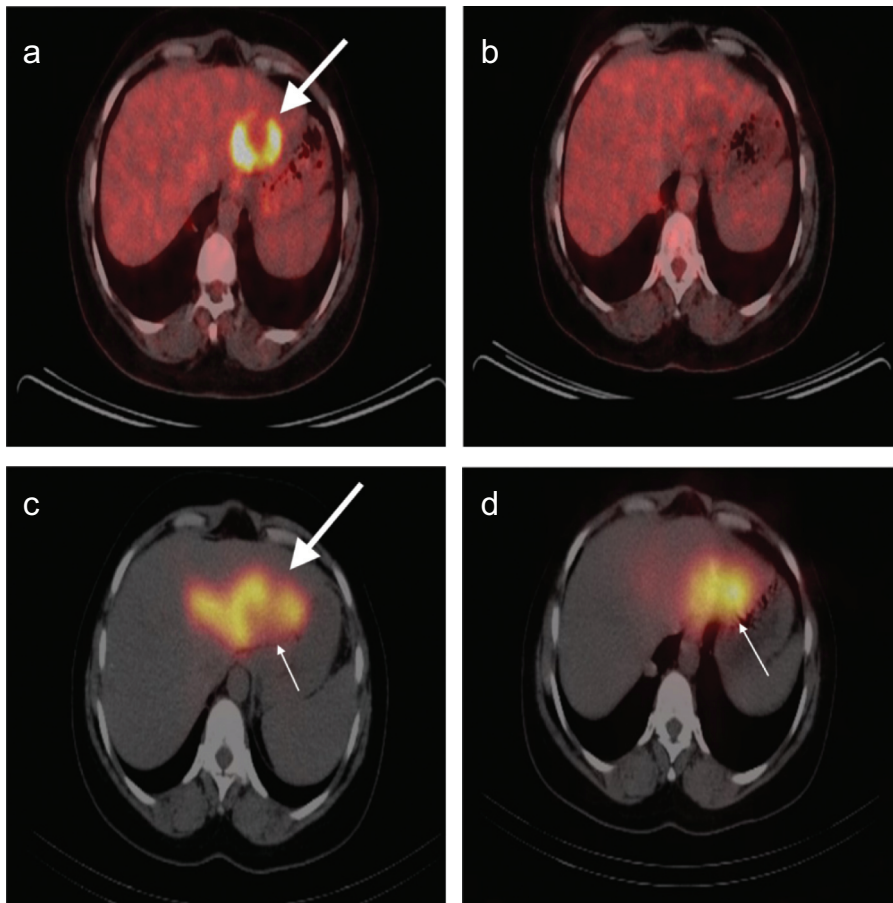


Figure 4. a-d. Patient case: A 59-year-old woman with colorectal cancer in segment 2. (a) ^{18}F -FDG PET/CT demonstrates dense FDG uptake in a peripheral rim and a central necrotic ametabolic area (arrow). (b) 3-month follow-up ^{18}F -FDG PET/CT image shows complete metabolic response. (c) HAPS SPECT/CT fusion images acquired before SIRT showing a heterogeneous perfusion pattern in a metastatic lesion in segment 2 with linear MAA uptake in segment 4A (thick arrow) but faint MAA uptake in the center of the tumor (thin arrow). (d) Bremsstrahlung image acquired after SIRT does not show linear MAA uptake in segment 4A but shows high microsphere distribution in the center of the tumor (thin arrow).

locregional therapy of liver tumors, whole-body scans with ^{18}F -FDG PET/CT can also detect extrahepatic metastases and inform treatment decisions, such as addition of systemic therapy. Distant metastases can occur during follow-up despite a primary tumor response, even in patients with HCC, which has a low incidence of extrahepatic metastasis.²⁹ This occurred in 3 of 68 patients with HCC. Additionally, two patients with liver tumor progression after SIRT developed extrahepatic metastases. ^{18}F -FDG PET/CT uptake may be able to identify patients with HCC who are more likely to have a poor prognosis.

Post-therapeutic dosimetry with bremsstrahlung SPECT/CT is a good complementary evaluation to confirm MAA findings. Because it corresponds to the real distribution of the therapeutic agent, it may more

accurately reflect the true dose and can be used to define tumoral threshold doses and liver maximal tolerated dose. However, both the heterogeneous distribution of microspheres within the intrahepatic vasculature and the anatomic attenuation of the broad energy spectrum of secondary bremsstrahlung x-ray radiation could limit the value of post-therapy bremsstrahlung scans in evaluating microsphere localization. Resulting HAPS images and bremsstrahlung images may be discordant, and dosimetry based on pretreatment images may not reflect the true exposure after SIRT. In our study, a discrepancy between imaging methods was observed in several patients, as demonstrated in patient case 1 (Figures 4c and 4d). The slight difference in particle sizes between $^{99\text{m}}\text{Tc}$ -MAA and ^{90}Y microspheres, differences in catheter

tip position and radiopharmaceutical reflux to peripheral vascular structures causing imaging artifacts during pretreatment planning angiography and SIRT might also contribute to calculation inconsistencies.

There are some limitations in the study. First, it is a nonrandomized retrospective study and there is no internal control group. Second, it is single-center study. Although our hospital is a tertiary care research hospital, it reflects the results of only one center. Third, our study group consists of patients of various disease stages and pathological types. Therefore, it has a heterogeneous cohort. Lastly, due to being a tertiary care hospital, the medical data of some patients who were referred from other institutions were absent.

In conclusion, tumoral lesions characterized by diffuse $^{99\text{m}}\text{Tc}$ -MAA uptake in HAPS SPECT/CT images were associated with longer median OS after ^{90}Y SIRT than tumors with heterogeneous uptake, though no significant differences were observed in tumor response rates between subgroups with diffuse and heterogeneous perfusion. Despite a statistically significant difference in OS between patients with diffuse and heterogeneous patterns, the number of patients with diffuse pattern was relatively small (44/216, 20.4%). Thus, SIRT remains an option regardless of MAA perfusion pattern. Nevertheless, assessment of tumor perfusion may still be useful to evaluate response to therapy. Further analyses are needed to better understand the full relation between these parameters and tumor biology.

Acknowledgments

The authors thank Sara Gardenghi, PhD; Jenny Cai, MSc; Alita Anderson, MD; Naomi Ruff, PhD; Adia Shy, PhD; Kathleen Labonge, MBA; and Edward Gloria of Eubio LLC for publication support for journal submission.

Conflict of interest disclosure

The authors declared no conflicts of interest.

References

1. Saxena A, Chua TC, Bester L, Kokandi A, Morris DL. Factors predicting response and survival after yttrium-90 radioembolization of unresectable neuroendocrine tumor liver metastases: A critical appraisal of 48 cases. *Ann Surg.* 2010;251(5):910-916. [Crossref]
2. Wasan HS, Gibbs P, Sharma NK, et al. First-line selective internal radiotherapy plus chemotherapy versus chemotherapy alone in patients with liver metastases from colorectal cancer (FOXFIRE, SIFLOX, and FOXFIRE-Global): A combined analysis of three multicentre, randomised, Phase 3 trials. *Lancet Oncol.* 2017;18(9):1159-1171. [Crossref]

3. Kennedy A. Radioembolization of hepatic tumors. *J Gastrointest Oncol*. 2014;5(3):178-189.
4. Sangro B, Inarrairaegui M, Bilbao JL. Radioembolization for hepatocellular carcinoma. *J Hepatol*. 2012;56(2):464-473. [\[Crossref\]](#)
5. Gong C, Ma G, Hu X, et al. Pretreatment ¹⁸F-FDG uptake heterogeneity predicts treatment outcome of first-line chemotherapy in patients with metastatic triple-negative breast cancer. *Oncologist*. 2018;23(10):1144-1152. [\[Crossref\]](#)
6. Li XF, Du Y, Ma Y, Postel GC, Civelek AC. 18F-Fluorodeoxyglucose Uptake and Tumor Hypoxia: Revisit 18F-Fluorodeoxyglucose in Oncology Application. *Transl Oncol*. 2014;7(2):240-247. [\[Crossref\]](#)
7. Civelek AC, Sitzmann JV, Chin BB, Venbrux A, Wagner HNJr, Grochow LB. Misperfusion of the liver during hepatic artery infusion chemotherapy: Value of preoperative angiography and postoperative pump scintigraphy. *AJR Am J Roentgenol*. 1993;160(4):865-870. [\[Crossref\]](#)
8. Padia SA, Lewandowski RJ, Johnson GE, et al. Radioembolization of hepatic malignancies: Background, quality improvement guidelines, and future directions. *J Vasc Interv Radiol*. 2017;28(1):1-15. [\[Crossref\]](#)
9. Lenoir L, Edeline J, Rolland Y, et al. Usefulness and pitfalls of MAA SPECT/CT in identifying digestive extrahepatic uptake when planning liver radioembolization. *Eur J Nucl Med Mol Imaging*. 2012;39(5):872-880. [\[Crossref\]](#)
10. Lambert B, Mertens J, Sturm EJ, Stienaers S, Defreyne L, D'Asseler Y. 99mTc-labelled macroaggregated albumin (MAA) scintigraphy for planning treatment with 90Y microspheres. *Eur J Nucl Med Mol Imaging*. 2010;37(12):2328-2333. [\[Crossref\]](#)
11. Hamami ME, Poeppel TD, Muller S, et al. SPECT/CT with 99mTc-MAA in radioembolization with 90Y microspheres in patients with hepatocellular cancer. *J Nucl Med*. 2009;50(5):688-692. [\[Crossref\]](#)
12. Gulec SA, Mesoloras G, Stabin M. Dosimetric techniques in 90Y-microsphere therapy of liver cancer: The MIRD equations for dose calculations. *J Nucl Med*. 2006;47(7):1209-1211.
13. Flamen P, Vanderlinden B, Delatte P, et al. Multimodality imaging can predict the metabolic response of unresectable colorectal liver metastases to radioembolization therapy with yttrium-90 labeled resin microspheres. *Phys Med Biol*. 2008;53(22):6591-6603. [\[Crossref\]](#)
14. Ulrich G, Dudeck O, Furth C, et al. Predictive value of intratumoral 99mTc-macroaggregated albumin uptake in patients with colorectal liver metastases scheduled for radioembolization with 90Y-microspheres. *J Nucl Med*. 2013;54(4):516-522. [\[Crossref\]](#)
15. Volkan-Salanci B, Bozkurt MF, Peynircioglu B, Cil B, Ugur O. The relation between perfusion pattern of hepatic artery perfusion scintigraphy and response to y-90 microsphere therapy. *Mol Imaging Radionucl Ther*. 2013;22(3):98-102. [\[Crossref\]](#)
16. Haug AR, Heinemann V, Bruns CJ, et al. 18F-FDG PET independently predicts survival in patients with cholangiocellular carcinoma treated with 90Y microspheres. *Eur J Nucl Med Mol Imaging*. 2011;38(6):1037-1045. [\[Crossref\]](#)
17. Sabet A, Ahmadzadehfah H, Muckle M, et al. Significance of oral administration of sodium perchlorate in planning liver-directed radioembolization. *J Nucl Med*. 2011;52(7):1063-1067. [\[Crossref\]](#)
18. Lau WY, Kennedy AS, Kim YH, et al. Patient selection and activity planning guide for selective internal radiotherapy with yttrium-90 resin microspheres. *Int J Radiat Oncol Biol Phys*. 2012;82(1):401-407. [\[Crossref\]](#)
19. Kao YH, Tan EH, Ng CE, Goh SW. Clinical implications of the body surface area method versus partition model dosimetry for yttrium-90 radioembolization using resin microspheres: A technical review. *Ann Nucl Med*. 2011;25(7):455-461. [\[Crossref\]](#)
20. Gaba RC, Lewandowski RJ, Hickey R, et al. Transcatheter therapy for hepatic malignancy: Standardization of terminology and reporting criteria. *J Vasc Interv Radiol*. 2016;27(4):457-473. [\[Crossref\]](#)
21. Young H, Baum R, Cremerius U, et al. Measurement of clinical and subclinical tumour response using [18F]-fluorodeoxyglucose and positron emission tomography: Review and 1999 EORTC recommendations. European Organization for Research and Treatment of Cancer (EORTC) PET study group. *Eur J Cancer*. 1999; 35(13):1773-1782. [\[Crossref\]](#)
22. Vilgrain V, Pereira H, Assenat E, et al. Efficacy and safety of selective internal radiotherapy with yttrium-90 resin microspheres compared with sorafenib in locally advanced and inoperable hepatocellular carcinoma (SARAH): An open-label randomised controlled phase 3 trial. *Lancet Oncol*. 2017; 18(12):1624-1636. [\[Crossref\]](#)
23. Chow PKH, Gandhi M, Tan SB, et al. SIRveNIB: Selective internal radiation therapy versus sorafenib in Asia-Pacific patients with hepatocellular carcinoma. *J Clin Oncol*. 2018;36(19):1913-1921. [\[Crossref\]](#)
24. Edeline J, Crouzet L, Campillo-Gimenez B, et al. Selective internal radiation therapy compared with sorafenib for hepatocellular carcinoma with portal vein thrombosis. *Eur J Nucl Med Mol Imaging*. 2016;43(4):635-643. [\[Crossref\]](#)
25. Vouche M, Habib A, Ward TJ, et al. Unresectable solitary hepatocellular carcinoma not amenable to radiofrequency ablation: Multicenter radiology-pathology correlation and survival of radiation segmentectomy. *Hepatology*. 2014;60(1):192-201. [\[Crossref\]](#)
26. Lewandowski RJ, Kulik LM, Riaz A, et al. A comparative analysis of transarterial downstaging for hepatocellular carcinoma: Chemoembolization versus radioembolization. *Am J Transplant*. 2009;9(8):1920-1928. [\[Crossref\]](#)
27. Braat AJ, Huijbregts JE, Molenaar IQ, Borel Rinkes IH, Van Den Bosch MA, Lam MG. Hepatic radioembolization as a bridge to liver surgery. *Front Oncol*. 2014;4:199. [\[Crossref\]](#)
28. Zhao Y, Liu C, Zhang Y, et al. Prognostic value of tumor heterogeneity on 18F-FDG PET/CT in HR+HER2- metastatic breast cancer patients receiving 500 mg fulvestrant: A retrospective study. *Sci Rep*. 2018;8(1):14458. [\[Crossref\]](#)
29. Senthilnathan S, Memon K, Lewandowski RJ, et al. Extrahepatic metastases occur in a minority of hepatocellular carcinoma patients treated with locoregional therapies: Analyzing patterns of progression in 285 patients. *Hepatology*. 2012;55(5):1432-1442. [\[Crossref\]](#)